X-Ray Directional Dichroism of a Polar Ferrimagnet

M. Kubota,[1,*] T. Arima,[1,2,†] Y. Kaneko,[1] J. P. He,[1] X. Z. Yu,[1] and Y. Tokura[1,3,4]

[1]*Spin Superstructure Project, ERATO, Japan Science and Technology Corporation, AIST Tsukuba Central 4, Tsukuba 305-8562, Japan*

[2]*Institute of Materials Science, University of Tsukuba, Tsukuba 305-8573, Japan*

[3]*Department of Applied Physics, University of Tokyo, Tokyo, 113-8656, Japan*

[4]*Correlated Electron Research Center (CERC), AIST Tsukuba Central 4, Tsukuba 305-8562, Japan*

(Received 4 September 2003; published 29 March 2004)

In a polar ferrimagnet $GaFeO_3$, we have found a novel magneto-optical effect, termed x-ray nonreciprocal directional dichroism (XNDD), that the x-ray absorption at around the K edge of an Fe ion depends on whether the x-ray propagation vector is parallel or antiparallel to the outer product of the magnetization and electric-polarization vectors. The XNDD spectroscopy as demonstrated here can be a useful tool to probe the local magnetism in noncentrosymmetric systems such as magnetic interfaces and nanostructures.

DOI: 10.1103/PhysRevLett.92.137401 PACS numbers: 78.70.Dm, 75.80.+q, 78.20.Ls

Left- and right-handed circularly polarized lights encounter a difference in the refractive index and/or absorption coefficient in a ferromagnetic solid when the magnetization is present parallel to the light propagation direction ($\boldsymbol{k}$ vector), as is well known as the Faraday effect. When the inversion symmetry is further broken in such a magnetic solid as possessing polarity or chirality, a novel magneto-optical effect, termed nonreciprocal directional dichroism (NDD) or magnetochiral dichroism, is expected to show up [1–3]. In the case of a polar ferromagnet (or ferrimagnet), for example, the NDD is described as the phenomenon that the light or x-ray absorption depends on whether the $\boldsymbol{k}$ vector is parallel or antiparallel to outer-product $\boldsymbol{P} \times \boldsymbol{M}$ under the preservation of mirror symmetry. ($\boldsymbol{P}$ and M denote the electric-polarization and spontaneous magnetization vectors, respectively.) In other words, the NDD distinguishes a front and a back side of a ferromagnetic (or ferrimagnetic) slab having the in-plane magnetization with respect to the $\boldsymbol{k}$ vector. Here we show the first observation of the NDD effect in the x-ray region for a polar ferrimagnet, $GaFeO_3$.

The NDD or related novel magneto-optical effect was first studied by Novikov and co-workers [4,5]. They confirmed the nonreciprocal directional birefringence in terms of the frequency splitting of oppositely propagating waves from a ring laser containing a polar nonmagnetic $LiIO_3$ crystal inside its resonator in an alternating magnetic field [4]. More than decade later, such a nonreciprocal effect was observed also in magnetic materials [6]. Recently, the nonreciprocal effects for visible light have been explored successfully by Rikken and co-workers for various antiferromagnetic and paramagnetic chiral compounds with the use of relatively high magnetic fields [7–11]. On the other hand, only a few studies [12,13] have been reported as yet on a nonreciprocal effect in x ray. Especially, there is no report, to the best of our knowledge, on x-ray nonreciprocal directional dichroism (XNDD) in a ferromagnet or a ferrimagnet. Taking full advantage of the element-specific nature of x-ray resonant spectroscopy, XNDD may be utilized as a useful tool to probe the magnetism in a noncentrosymmetric system such as biomaterial, interface, or artificial nanostructure.

We have adopted $GaFeO_3$ as a good candidate that can show the XNDD effect. $GaFeO_3$ is a rare example of the compounds, in which spontaneous polarization and magnetization coexist [14]. Electric polarization is generated along the b axis [15,16], while a magnetic easy axis is parallel to the c axis [16,17] [see Fig. 1(a)]. A $GaFeO_3$ crystal rod was grown by a floating zone method. A thin platelike specimen ($1.8 \times 1.8 \times 0.034$ mm^3) with (100) surfaces was cut from the crystal rod. Figure 1(b) shows the experimental configuration. The measurements were carried out at the beam line 1A at the Photon Factory in KEK, Japan. A synchrotron x-ray beam was monochromated by a pair of Si(111) crystals and injected on the $GaFeO_3$ $(\bar{1}00)$ surface. Typical resolution of the photon energy was $\sim$2 eV. Intensity of an incident I_0 and a transmission I_1 beam was measured with ionization chambers. In this study, we observed the change in absorption with the magnetization reversal, since XNDD is the change with a reversal of any of $\boldsymbol{k}$, $\boldsymbol{P}$, and M. A sinusoidal magnetic field with an amplitude of 50 mT and a frequency f of 10 Hz was applied along the c axis in order to reverse M. The modulation of transmission with the alternating magnetic field [$\Delta I_1(f)$, $\Delta I_1(2f)$, or $\Delta I_1(3f)$] was detected with a lock-in amplifier. Spectra of absorption μt and XNDD $\Delta \mu t$ were calculated from $I_1(dc)/I_0(dc)$ and $\Delta I_1(f)/I_1(dc)$, respectively.

Figure 2(a) exhibits x-ray absorption spectra of $GaFeO_3$ at 50 K in the vicinity of Fe K edge for the polarizations of x ray (E^{ω}) parallel to b and c. A bump at about 7.113 keV corresponds to transitions from Fe 1s to Fe 3d (preedge), while a local maximum at about

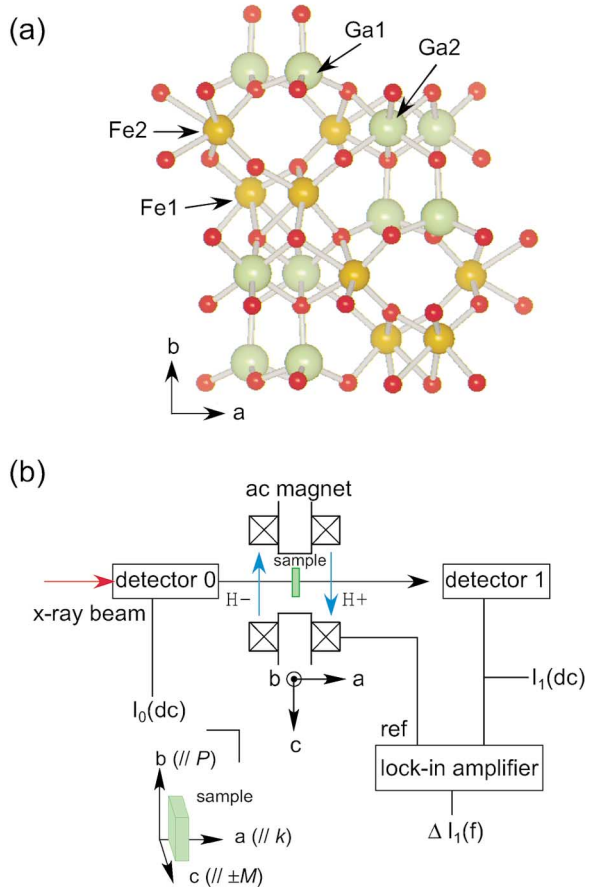

FIG. 1 (color). (a) Structure of a $GaFeO_3$ crystal with a space group of $Pc2_1n$. An electric polarization appears along the screw b axis, which causes the breaking of inversion symmetry. The magnetic structure is ferrimagnetic with a magnetic point group of $m'2'm$ below T_C (~ 205 K). The c axis is a magnetic easy axis and a saturated moment is about $0.6\mu_B$/Fe. (b) Experimental configuration for the observation of x-ray nonreciprocal directional dichroism (XNDD). A synchrotron x-ray beam was monochromated by a pair of Si(111) crystals. The x-ray beam is injected onto the $(\bar{1}00)$ plane, while an alternating magnetic field is applied along the c axis in Voigt configuration, with an amplitude of 50 mT and a frequency of 10 Hz. Ionization chambers were used for the detection of an incident intensity (I_0) and a transmission (I_1). XNDD was observed as the first-harmonic component of the transmission [$\Delta I_1(f)$] responding to the magnetic field with a lock-in amplifier.

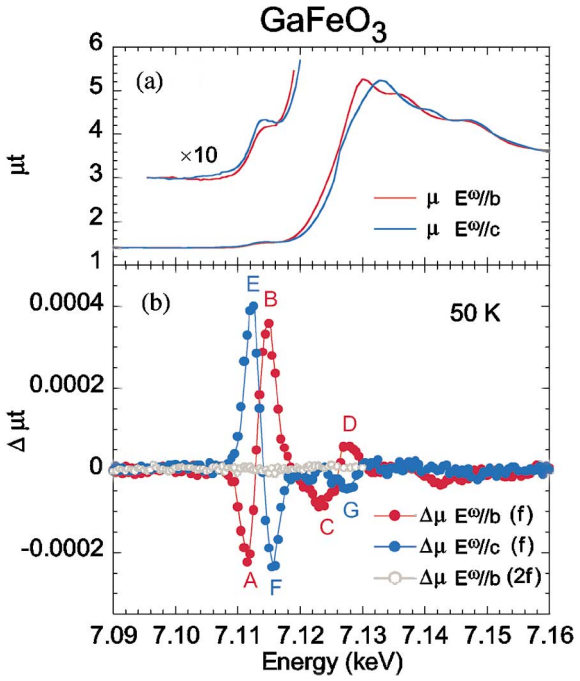

FIG. 2 (color). Spectra of (a) the x-ray absorption μt and (b) the XNDD $\Delta\mu t$ of a $GaFeO_3$ crystal at 50 K for $E^\omega \parallel b$ (red) and $E^\omega \parallel c$ (blue). $\Delta\mu t$ is defined as the difference of absorption coefficients when a magnetic field is applied parallel ($H+$) and antiparallel ($H-$) to the c axis. In (b) the spectrum of the second-harmonic component of the magnetic-field modulation for $E^\omega \parallel c$ is also shown with open circles.

7.130 keV corresponds to transitions from Fe $1s$ to Fe $4p$ (main edge). Spectra of XNDD at 50 K are shown in Fig. 2(b). As expected, absorption varies with the reversal of M in the Voigt configuration ($\boldsymbol{k} \perp \boldsymbol{H} \parallel c$). The magnitudes of XNDD around the preedge are comparable for $E^\omega \parallel b$ and $E^\omega \parallel c$, while the sign is opposite. XNDD is much larger around the preedge than around the main edge for the both x-ray polarizations. This indicates that the quadrupole transition from Fe $1s$ to Fe $3d$ plays an important role in this novel phenomenon.

The observed XNDD signal is clearly distinguished from conventional magneto-optical effects such as the Cotton-Mouton effect and x-ray magnetic circular dichroism (XMCD). The former effect that is proportional to $\boldsymbol{M}^2$ would appear as the second-harmonic component of the magnetic modulation signal. In this study the $2f$-modulation component was hardly observed as shown by open circles in Fig. 2(b). Therefore, the possibility is excluded that the observed signal of the first-harmonic component would be caused by the Cotton-Mouton effect, even if possible asymmetry of an applied magnetic field were taken into account. The XMCD signal should not be observed in the Voigt configuration of an external magnetic field, combined with a linearly polarized x-ray beam. In order to deny completely the possibility of XMCD, we also performed the modulation measurement in the condition that the direction of an applied magnetic field was tilted by $\pm 10°$ around the b axis. The observed $\Delta\mu t$ did not revert in sign with the tilting of the field direction. This indicates that the observed modulation in absorption is derived from the genuine Voigt component of a magnetic field.

The XNDD effect becomes weaker with increasing temperature as shown in Fig. 3(a). In Fig. 3(b) the XNDD magnitude is compared with M at a static magnetic field of 50 mT at respective temperatures. The temperature dependence of XNDD is similar to the behavior

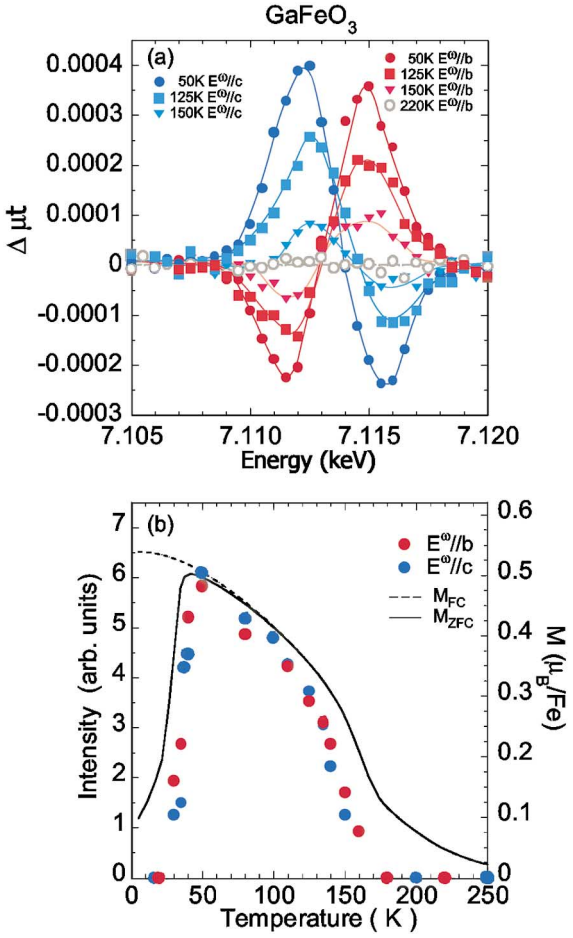

FIG. 3 (color). Temperature dependence of (a) the XNDD spectra in the pre-edge, and (b) the peak height of XNDD spectrum for $E^\omega \parallel b$ (red) and $E^\omega \parallel c$ (blue). The temperature dependence of the magnetization is also shown in (b) for comparison, which was measured in a static magnetic field of 50 mT along the c axis after a zero field cooling process (a solid line) and in the field cooling run (a broken line). The magnitude of XNDD as detected by a modulation field of 50 mT shows a similar temperature dependence of the magnetization taken after the zero-field cooling. At low temperatures, the magnetization cannot be reversed by the ac magnetic field because the coercive force of $GaFeO_3$ exceeds 50 mT below 40 K.

of M after zero-field cooling. (The decrease of the XNDD signal below 40 K is simply due to the insufficient magnetic field to reverse M.) This result is consistent with the feature that the XNDD signal should be proportional to M. In addition, the third-harmonic component $\Delta I(3f)$ was observed to be 24% as large at 50 K as that of the first-harmonic component. Because of a nonlinear magnetization curve, the magnetization changes approximately as a rectangular wave in a sinusoidal magnetic field. The $3f$ component is anticipated to be $1/3$ as large as the f component in the rectangular-wave limit, provided that the modulation of absorption is linear to M. The obtained value fairly agrees with this expectation.

Next we discuss spectra of XNDD. The integral of each XNDD spectrum over the Fe K-edge region is nearly zero, as shown in Fig. 2(b). This sum rule suggests that the transfer of spectral weight between Fe and other atoms is negligible and, hence, that the XNDD spectra can be well interpreted in terms of a single Fe-cluster model. First, we consider an Fe site surrounded by six oxygen ions as shown by the bonds in Fig. 1(a). Taking account of the feature that XNDD is the change in optical constant with the sign reversal of $\boldsymbol{k} \cdot (\boldsymbol{P} \times \boldsymbol{M})$, the most probable origin of XNDD is the interference between electric dipole ($E1$) and quadrupole ($E2$) processes through a spin-orbit coupling $\lambda \boldsymbol{L} \cdot \boldsymbol{S}$ and a breaking of the parity through the noncentrosymmetric crystal structure. In Fig. 4 the x-ray absorption processes for the configurations of $E^\omega \parallel b$ and $E^\omega \parallel c$ are schematically drawn. Only the relevant Fe states are displayed in this diagram. Here we take local coordinates x, y, and z parallel to the lattice vectors a, b, and c, respectively. Fe $3d$ states are split into e (approximate $3d_{xy}$ and $3d_{yz}$) and t (approximate $3d_{3y^2-r^2}$, $3d_{zx}$, and $3d_{z^2-x^2}$) states in an O crystal field. Because of the electric polarization along the b axis (E_y^{loc}), $3d_{xy}$, $3d_{3y^2-r^2}$, and $3d_{yz}$ states are hybridized with $4p_x$, $4p_y$, and $4p_z$ states, respectively. From the comparison of absorption spectra for $E^\omega \parallel b$ and $E^\omega \parallel c$ in Fig. 2(a), the $4p_y$ state locates 3 eV lower than $4p_z$. In the ground state, Fe^{3+} has a high-spin state with the magnetic easy-axis along c ($S = \frac{5}{2}$, $S_z = \pm\frac{5}{2}$). Since the spin state should not change upon either $E1$ or $E2$ transition, only the L_zS_z component in a spin-orbit coupling is crucial for the interference.

Local peaks of A–G in Fig. 2(b) are assigned to the transitions from $1s$ to $3d_{3y^2-r^2}$, $3d_{xy}$, $4p_y$, $4p_x$, $3d_{zx}$, $3d_{yz}$, and $4p_z$, respectively. As for $E^\omega \parallel b$ and $k \parallel a$, the intra-atomic $E2$ transition from Fe $1s$ to $3d_{xy}$ and the intra-atomic $E1$ transition from Fe $1s$ to $3d_{3y^2-r^2}$ hybridized with $4p_y$ interfere with each other, while for $E^\omega \parallel c$, so do the $E2$ transition to $3d_{zx}$ and the $E1$ transition to $3d_{yz}$ hybridized with $4p_z$. In this model, the XNDD at A and B (E and F) is caused by a transfer of spectral weight between the $E1$ and $E2$ transitions through L_zS_z. The splitting between A and B (E and F) peaks seems to be a little larger than the well-known crystal field splitting ($10Dq$) in an FeO_6 cluster [18], which is partly due to the lower local symmetry at the Fe sites. The sign reversal of XNDD at the preedge for $E^\omega \parallel b$ and $E^\omega \parallel c$ would originate from the difference in sign of $\langle 3d_{3y^2-r^2}|E_y^{\mathrm{loc}}|4p_y\rangle$ and $\langle 3d_{yz}|E_y^{\mathrm{loc}}|4p_z\rangle$. The simplest estimation of XNDD from the value of $\frac{\lambda}{10Dq}$ is of the order of 10^{-2}, which agrees well with the experimental result. The ratio of the XNDD at the preedge to the relevant $1s$–$3d$ absorption corrected by the subtraction of background is as large as about 1% in both the x-ray polarizations, $E^\omega \parallel b$ and $E^\omega \parallel c$. In this cluster model, the spectral weight at the main edge is also affected by the $E1$–$E2$ interference through the spin-orbit interaction as shown in Fig. 4. However, the less

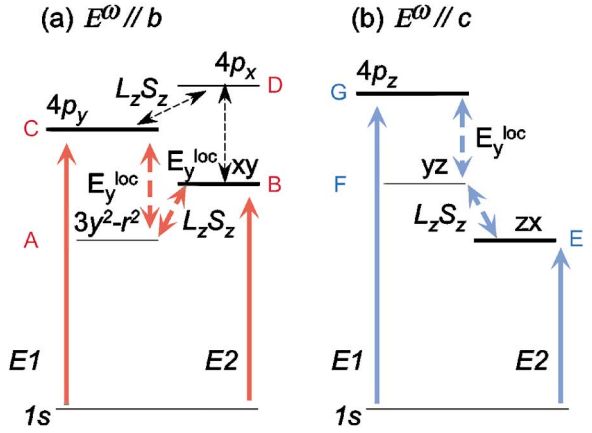

FIG. 4 (color). Processes relevant to the microscopic origin of the XNDD effect in $GaFeO_3$ for (a) $E^\omega \parallel b$ and (b) $E^\omega \parallel c$. In the vicinity of Fe K absorption edge, both the electric dipole ($E1$) process from Fe $1s$ to Fe $4p$ and the electric quadrupole ($E2$) process from Fe $1s$ to Fe $3d$ appear. For $E1$–$E2$ interference, spin-orbit coupling and breaking symmetry of b mirror is crucial. The A–G indices of $3d$ and $4p$ levels correspond with the A–G peaks of XNDD spectra shown in Fig. 2(a), respectively. See text.

localized $4p$ states form a broad conduction band, and the effect of spin-orbit interaction in $4p$ should be much weaker than that in the localized $3d$. In fact, the observed XNDD peaks at about preedge are at least 5 times as large as the C and D. The small intensity of G is also explained in the model, because the $\lambda L_z S_z$ term does not modulate the $4p_z$ state directly.

The aforementioned $E1$–$E2$ interference should occur at all the Fe sites. In $GaFeO_3$, Fe ions mainly occupy Fe1 and Fe2 sites. The spin moments at the two sites are opposite in direction in this ferrimagnetic compound [16,19,20], yet the local electric polarizations are also opposite between Fe1 and Fe2 sites as shown in Fig. 2 [16,20]. Thus the XNDD terms at Fe1 and Fe2 sites reinforce each other.

The present XNDD on $GaFeO_3$ is roughly governed by the spontaneous magnetization, because every magnetic ion occupies a noncentrosymmetric site. The technique is even more powerful to study ferromagnets that contain both centrosymmetric and noncentrosymmetric magnetic sites. One typical example is magnetoresistive heterostructure where the interface magnetism plays the most important role in tunneling magnetoresistance behavior. The possibly different temperature- and magnetic-field dependence in magnetism between interface and bulk can be investigated by using the XNDD-related method. In addition, XNDD is an element-selective magnetic probe like XMCD. The XNDD effect can be a useful technique to detect magnetism of a specified element at noncentrosymmetric sites selectively.

The authors gratefully acknowledge H. Sawa and R. Kumai for the development of the beam line 1A at the Photon Factory in KEK, and S. Murakami and N. Nagaosa for stimulating discussions.

*Present address: Photon, Factory, Institute of Materials Structure Science, KEK, Tsukuba, 305-0801, Japan. Electronic address: mkubota@post.kek.jp
†To whom correspondence should be addressed. Electronic address: arima@ims.tsukuba.ac.jp

[1] W. F. Brown, Jr., S. Shtrikman, and D. Treves, J. Appl. Phys. **34**, 1233 (1963).
[2] R. M. Hornreich and S. Shtrikman, Phys. Rev. **171**, 1065 (1968).
[3] R. V. Pisarev, Zh. Eksp. Teor. Fiz. **58**, 1421 (1970) [Sov. Phys. JETP **31**, 761 (1970)].
[4] V. A. Markelov, M. A. Novikov, and A. A. Turkin, Pis'ma Zh. Eksp. Teor. Fiz. **25**, 404 (1977) [JETP Lett. **25**, 378 (1977)].
[5] E. L. Bubis and M. A. Novikov, Zh. Tekh. Fiz. **52**, 399 (1982) [Sov. Phys. Tech. Phys. **27**, 257 (1982)].
[6] B. B. Krichevtsov, V. V. Pavlov, R. V. Pisarev, and V. N. Gridnev, J. Phys. Condens. Matter **5**, 8233 (1993).
[7] G. L. J. A. Rikken and E. Raupach, Nature (London) **390**, 493 (1997).
[8] G. L. J. A. Rikken and E. Raupach, Nature (London) **405**, 932 (2000).
[9] G. L. J. A. Rikken and E. Raupach, Phys. Rev. E **58**, 5081 (1998).
[10] G. L. J. A. Rikken, J. Folling, and P. Wyder, Phys. Rev. Lett. **87**, 236602 (2001).
[11] T. Roth and G. L. J. A. Rikken, Phys. Rev. Lett. **88**, 063001 (2002).
[12] J. Goulon, A. Rogalev, C. Goulon-Ginet, G. Benayoun, and L. Paolasini, Phys. Rev. Lett. **85**, 4385 (2000).
[13] J. Goulon, A. Rogalev, F. Wilhelm, C. Goulon-Ginet, and P. Carra, Phys. Rev. Lett. **88**, 237401 (2002).
[14] J. P. Remeika, J. Appl. Phys. Suppl. **31**, 263S (1960).
[15] E. A. Wood, Acta Crystallogr. **13**, 682 (1960).
[16] S. C. Abrahams, J. M. Reddy, and J. L. Bernstein, J. Chem. Phys. **42**, 3957 (1965).
[17] C. H. Nowlin and R. V. Jones, J. Appl. Phys. **34**, 1262–1263 (1963).
[18] R. V. Pisarev, Fiz. Tverd. Tela **7**, 207 (1965) [Sov. Phys. Solid State **7**, 158 (1965)].
[19] R. B. Frankel and N. A. Blum, Phys. Rev. Lett. **15**, 958 (1965).
[20] A. Delapalme, J. Phys. Chem. Solids **28**, 1451 (1967).